Intramolecular Charge Transfer and Dielectric Solvent Relaxation in *n*-Propyl Cyanide. *N*-Phenylpyrrole and 4-Dimethylamino-4′-cyanostilbene

Sergey I. Druzhinin,*,† Victor A. Galievsky,‡ Toshitada Yoshihara,§ and Klaas A. Zachariasse*

Max-Planck-Institut für biophysikalische Chemie, Spektroskopie und Photochemische Kinetik, 37070 Göttingen, Germany

Received: August 15, 2006; In Final Form: September 19, 2006

Fast intramolecular charge transfer (ICT) accompanied by dual fluorescence from a locally excited (LE) and an ICT state taking place with *N*-phenylpyrrole (PP) in the solvent *n*-propyl cyanide (PrCN) is investigated as a function of temperature between 25 and −112 °C. The LE and ICT fluorescence decays from −45 to −70 °C can be adequately fitted with two exponentials, in accordance with a two state (LE + ICT) reaction mechanism, similar to what has been observed with PP in the more polar and less viscous alkyl cyanides acetonitrile (MeCN) and ethyl cyanide (EtCN). At lower temperatures, triple-exponential fits are required for the LE and ICT decays. The ICT emission band maximum of the time-resolved fluorescence spectra of PP in PrCN at −100 °C displays a spectral shift from 29 230 cm^{-1} at $t = 0$ to 27 780 cm^{-1} at infinite time, which equilibration process is attributed to dielectric solvent relaxation. From the time dependence of this shift, in global analysis with that of the band integrals BI(LE) and BI(ICT) of the time-resolved LE and ICT fluorescence bands, the decay times 119 and 456 ps are obtained. Dielectric relaxation times of 20 and 138 ps are determined from the double-exponential spectral solvation response function $C(t)$ of the probe molecule 4-dimethylamino-4′-cyanostilbene in PrCN at −100 °C. It is concluded from the similarity of the times 119 ps (PP) and 138 ps (DCS) that the deviation from double-exponential character for the fluorescence decays of PP in PrCN below −70 °C is due to the interference of dielectric solvent relaxation with the ICT reaction. This fact complicates the kinetic analysis of the LE and ICT fluorescence decays. The kinetic analysis for PP in PrCN is hence restricted to temperatures between −70 and −45 °C. From this analysis, the forward and backward ICT activation energies E_a (12 kJ/mol) and E_d (17 kJ/mol) are obtained, giving an ICT stabilization enthalpy $-\Delta H$ of 5 kJ/mol. A comparison of the reaction barriers for PP in the three alkyl cyanides PrCN, EtCN, and MeCN (*J. Phys. Chem. A* **2005**, *109*, 1497) shows that E_a becomes smaller with increasing solvent polarity (from 12 to 6 kJ/mol), whereas E_d remains effectively constant. Both observations are indicative of a late transition state for the LE → ICT reaction. The significance of the Leffler−Hammond postulate in this connection is discussed: not primarily the energy of the LE, ICT, and transition states but rather the extent of charge transfer in these states determines whether an early or a late transition state is present.

Introduction

N-Phenylpyrrole (PP) undergoes fast intramolecular charge transfer (ICT) in sufficiently polar solvents such as the alkyl cyanides.[1−4] Apart from these experimental investigations, theoretical treatments of this process have appeared.[5−7] Recently, the ICT reaction dynamics and thermodynamics of PP in acetonitrile (MeCN) and ethyl cyanide (EtCN) were determined as a function of temperature.[4] The fluorescence decays of the locally excited (LE) and ICT states are double-exponential and a single-exponential decay results from the LE/ICT analysis, in which the ICT decay is deconvoluted with that of the LE.[4] Both observations are in accordance with a two-state (LE and ICT) reaction mechanism. In the case of PP in *n*-propyl cyanide (PrCN) as the solvent, however, it was found that three exponentials are needed to fit the LE and ICT fluorescence decays at temperatures below −70 °C. An investigation of this phenomenon, invoking solvent dielectric relaxation operating alongside ICT, is presented here.

To obtain independent information on the dielectric solvent relaxation of PrCN, time-resolved fluorescence spectra at temperatures between −45 and −110 °C in this solvent are measured by employing 4-dimethylamino-4′-cyanostilbene (DCS) as a probe molecule. This molecule is a reliable probe, due to the fact that only one singlet excited state governs its photophysics. It has been established that an ICT reaction accompanied with dual fluorescence does not take place with DCS, neither in nonpolar nor in polar solvents.[8−12] Contrary to these experimental observations that dual (LE + ICT) fluorescence is absent, it has recently been concluded from ab initio CASSCF calculations that a twisted ICT state is formed from the initially excited state of this molecule.[13]

In addition to the treatment of the impact of solvent relaxation, thermodynamic data such as the forward and backward reaction barriers and the stabilization enthalpy ΔH for the ICT reaction of PP in PrCN at temperatures above −70 °C are determined and the results are compared with those found previously in the more polar alkyl cyanides EtCN and MeCN.[4]

* Corresponding authors. Fax: +49-551-201-1501. E-mail: sdruzhi@gwdg.de (S.I.D.), kzachar@gwdg.de (K.A.Z.).

† Affiliation: Chemical Department, Moscow State University, 119899 Moscow, Russia.

‡ Present address: Institute of Molecular and Atomic Physics, National Academy of Sciences of Belarus, 220072 Minsk, Belarus.

§ Present address: Department of Chemistry, Gunma University, Kiryu, Gunma 376-8515, Japan.

10.1021/jp0652547 CCC: $33.50
Published on Web 11/07/2006

Experimental Section

PP (from Aldrich) was purified by column chromatography (Al_2O_3). The synthesis of DCS has been reported previously.[9] For both compounds, HPLC was the last purification step. The solvent PrCN (butyronitrile, Merck, for analysis) was chromatographed over Al_2O_3 just prior to use. The solutions, with an optical density between 0.4 and 0.6 for the maximum of the lowest-energy band in the absorption spectrum (concentration around 2×10^{-4} M), were deaerated by bubbling with nitrogen for 15 min.

The fluorescence spectra were measured with a quantum-corrected modified[14] Fluoromax 3 spectrofluorometer. The fluorescence decay times of PP were determined with a picosecond single photon counting (SPC) system (excitation wavelength λ_{exc}: 276 nm), consisting of a mode-locked titanium-sapphire laser (Coherent, MIRA 900-F) pumped by an argon ion laser (Coherent, Innova 415).[4,14] The instrument response function has a full width at half-maximum (fwhm) of around 19 ps. Two time ranges are routinely employed simultaneously: here 2 and 10 ps/channel, in 1650 and 1850 effective channels, respectively. The analysis procedure of the fluorescence decays has been described previously.[15,16]

The fluorescence decays of DCS in PrCN were obtained with an SPC setup consisting of an argon ion laser (Coherent Innova Sabre R-TSM-10 with APE modelocker), a dye laser (Coherent 701-1CD; Rhodamine 6G), and a frequency doubler (BBO, 298 nm).[17] The instrument response function has a fwhm of 26 ps. The concentration of DCS was around 3×10^{-5} M. For the determination of the solvent relaxation times from the spectral shift of the DCS fluorescence band maximum, the fluorescence decays (monochromator slit width 6 nm) were measured at 10 nm intervals with a resolution of 2 ps/channel or 0.5 ps/channel (for -45 °C). The longer decay time originating from the 10 ps/channel decays is taken as a constant in the analysis of the 0.5 ps/channel decays. Each decay is fitted to an *n*-exponential function ($n = 2$ or 3, depending on the wavenumber $\tilde{\nu}$) for the purpose of deconvolution and removal of noise.

Results and Discussion

Absorption and Fluorescence Spectra of PP in PrCN. The absorption spectra of PP in PrCN, shown in Figure 1, consist of a broad and structureless band, with a maximum $\tilde{\nu}^{max}$(abs) at 39 320 cm^{-1} at 25 °C and 39 100 cm^{-1} at -112 °C (Table 1). This red-shift is caused by the increase of the solvent polarity (dielectric constant and refractive index) upon cooling, see Table 1. A similar polarity influence has been reported for PP in the more polar alkyl cyanides acetonitrile (MeCN) and ethyl cyanide (EtCN).[4]

An ICT reaction takes place in PrCN over the entire temperature range from 25 to -112 °C, as can be seen from fluorescence spectra of PP in Figure 1, separated into their LE and ICT components. The ICT/LE fluorescence quantum yield ratio Φ'(ICT)/Φ(LE) of PP in PrCN is rather small (0.18) at 25 °C,[18] as compared with 0.42 in MeCN,[4] but increases substantially upon cooling, reaching a value of 0.50 at -112 °C (Table 1). As a result of the cooling, the maximum $\tilde{\nu}^{max}$(ICT) of the ICT band shifts to the red from 28 920 to 27 530 cm^{-1}, between 25 and -112 °C, again a consequence of the increasing solvent polarity: the dielectric constant ϵ increases from 24.1 to 59.6, whereas the refractive index *n* changes from 1.382 to 1.448 over this temperature range.[19,20] From a comparison of the $\tilde{\nu}^{max}$(ICT) for PP in MeCN (27 530 cm^{-1}, $\epsilon = 50.2$) and in EtCN (28 030 cm^{-1}, $\epsilon = 39.0$) at -45 °C,[4] with those in PrCN at the corresponding ϵ values (27 710 cm^{-1} at -93.8 °C ($\epsilon = 50.3$) and 28 040 cm^{-1} at -61.1 ° C ($\epsilon = 39.0$)), it is seen that the energy of $\tilde{\nu}^{max}$(ICT) is largely determined by the dielectric constant rather than by the specific molecular nature of the solvent.

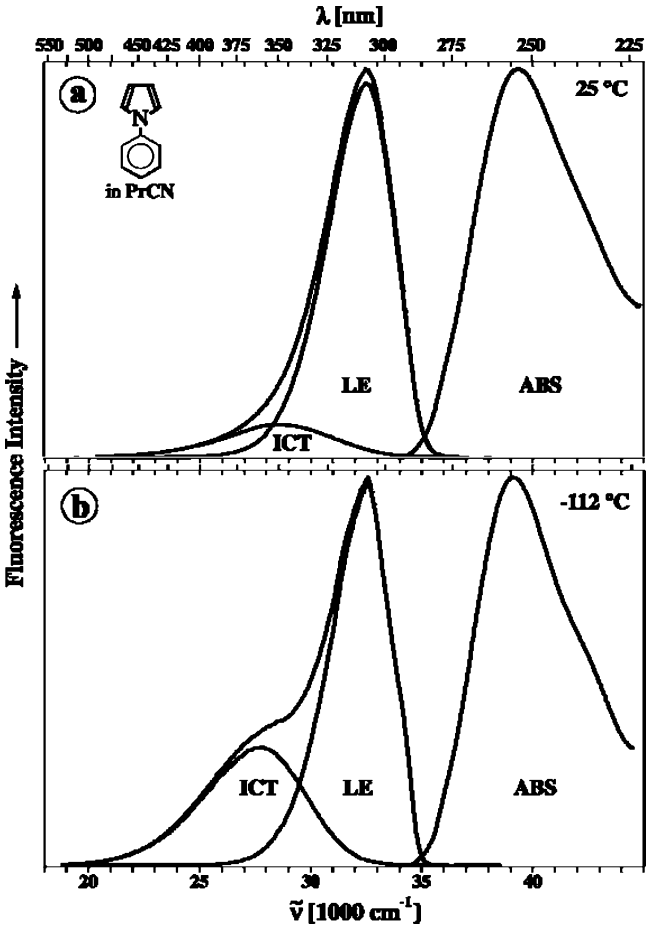

Figure 1. Absorption and fluorescence spectra ($\lambda_{exc} = 270$ nm) of *N*-phenylpyrrole (PP) in *n*-propyl cyanide (PrCN) at (a) 25 °C and (b) -112 °C. For the separation of the overall fluorescence spectrum into the LE and ICT components, the ICT emission spectrum of 4-cyano-*N*-phenylpyrrole (PP4C) in PrCN at both temperatures has been employed as a model for ICT, see ref 18.

TABLE 1: Data for *N*-Phenylpyrrole (PP) in *n*-Propyl Cyanide (PrCN) at Various Temperatures

T (°C)	ϵ^a	$n_D{}^b$	$\tilde{\nu}^{max}$(abs)^c [1000 cm^{-1}]	$\tilde{\nu}^{max}$(LE)^d [1000 cm^{-1}]	$\tilde{\nu}^{max}$(ICT)^e [1000 cm^{-1}]	$E(S_1)^f$ [1000 cm^{-1}]	Φ'(ICT)/Φ(LE)^g
25	24.1	1.382	39.32[h]	32.52	28.92	35.11	0.18
−45	35.1	1.416	39.23	32.55	28.23	35.05	0.25
−100	53.1	1.443	39.14	32.51	27.64	35.98	0.52
−110	58.4	1.447	39.10	32.51	27.55	34.99	0.52
−112[i]	59.6	1.448	39.10	32.52	27.53	34.99	0.50

[a] Dielectric constant, from ref 19. [b] Refractive index n_D, from ref 20. [c] Absorption maximum. [d] Maximum of the LE fluorescence band. [e] Maximum of the ICT fluorescence band. [f] Crossing of absorption and fluorescence spectrum. Due to the overlap of the S_1 and S_2 bands in the absorption spectrum, $E(S_1)$ is an approximation, giving at least some indication of the lowering of the S_1 energy of PP with decreasing temperature, i.e, with increasing solvent polarity. [g] ICT/LE fluorescence quantum yield ratio. [h] Extinction coefficient 13 320 M^{-1} cm^{-1}. [i] Melting point PrCN: -112 °C.

LE and ICT Fluorescence Decays of PP in PrCN as a Function of Temperature. With PP in PrCN at -45 °C, the LE and ICT fluorescence decays i_f(LE) and i_f(ICT) are double exponential (eqs 1−3, $\tau_2 < \tau_1$), with decay times $\tau_2 = 31$ ps and $\tau_1 = 7.38$ ns and an amplitude ratio $A_{12}/A_{11} = 0.72$.[4] This double-exponential character shows that two interconverting

SCHEME 1

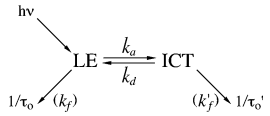

excited states are sufficient to describe the excited-state reaction: LE and ICT (Scheme 1). In accordance with this interpretation, the ICT decay deconvoluted with that of the LE state (LE/ICT decay, eq 4) is single exponential, with a decay time τ(LC) of 55.9 ps.[4]

$$i_f(\mathrm{LE}) = A_{11}\exp(-t/\tau_1) + A_{12}\exp(-t/\tau_2) \quad (1)$$

$$i_f(\mathrm{ICT}) = A_{21}\exp(-t/\tau_1) + A_{22}\exp(-t/\tau_2) \quad (2)$$

$$A = A_{12}/A_{11} = (k_a + 1/\tau_0(\mathrm{LE}) - 1/\tau_1)/(1/\tau_2 - k_a - 1/\tau_0(\mathrm{LE})) \quad (3)$$

$$\tau(\mathrm{LC}) = 1/(k_d + 1/\tau'_0(\mathrm{ICT})) \quad (4)$$

In Scheme 1, k_a and k_d are the rate constants of the forward and backward ICT reaction, and τ_0(LE) and τ'_0(ICT) are the fluorescence lifetimes (no reaction) of the LE and ICT state, whereas k_f(LE) and k'_f(ICT) are the radiative rate constants.

Double and Triple-Exponential Fluorescence Decays. The LE and ICT fluorescence decays of PP in PrCN, measured at wavelengths at which either only LE (303 nm) or ICT (400 nm) fluorescence occurs (see Figure 1), can be fitted with two exponentials, as already documented above for −45 °C.[4] These measurements have been made from 5 °C (τ_2 = 7.5 ps, τ_1 = 6.30 ns) down to around −70 °C (τ_2 = 64 ps, τ_1 = 7.34 ns). At lower temperatures, such as at −85 °C, however, the LE and ICT fluorescence decays of PP in PrCN cannot be fitted adequately with two exponentials. Three exponentials (τ_3, τ_2, τ_1) are required at this temperature (eqs 5 and 6), as shown in Figure 2. This behavior is found over the entire temperature range between −75 and −112 °C, the melting point of the solvent (Figure 2b). A plot of the three decay times and the corresponding amplitude ratios A_{13}/A_{11} and A_{12}/A_{11} is presented in Figure 3.

$$i_f(\mathrm{LE}) = A_{11}\exp(-t/\tau_1) + A_{12}\exp(-t/\tau_2) + A_{13}\exp(-t/\tau_3) \quad (5)$$

$$i_f(\mathrm{ICT}) = A_{21}\exp(-t/\tau_1) + A_{22}\exp(-t/\tau_2) + A_{23}\exp(-t/\tau_3) \quad (6)$$

In support of this observation of triple-exponential LE and ICT decays, the LE/ICT decays of PP in PrCN at temperatures below −70 °C are no longer single exponential, but can be fitted as double exponentials, with decay times 149 and 417 ps at −85 °C (2 ps/channel) and 519 and 3216 ps at −112 °C (10 ps/channel), as examples.

Picosecond Fluorescence Decays of PP in PrCN at −100 °C. To investigate the reason for this deviation from the double-exponential behavior as required by the presence of two excited states LE and ICT in the reaction mechanism (Scheme 1),[4] fluorescence decays were measured for PP in PrCN at −100 °C over the entire LE + ICT spectral range, see Figure 1b, from 288 to 420 nm (19 different wavelengths). Three representative decays, at 292 (LE), 344 (LE + ICT), and 410 (ICT) nm, are shown in Figure 4. For all these decay curves, three exponentials are needed for an acceptable fit, with decay times similar to those obtained from a global analysis of the LE and ICT decays at wavelengths at which either only LE (303 nm) or ICT (400 nm) emits (τ_3 = 173 ps, τ_2 = 514 ps, τ_1 = 7360 ps with A_{13}/A_{11} = 0.71 and A_{12}/A_{11} = 1.36, see Figure 3 and Figure S1 in the Supporting Information). The resulting time-resolved LE and ICT fluorescence spectra are presented in the following section.

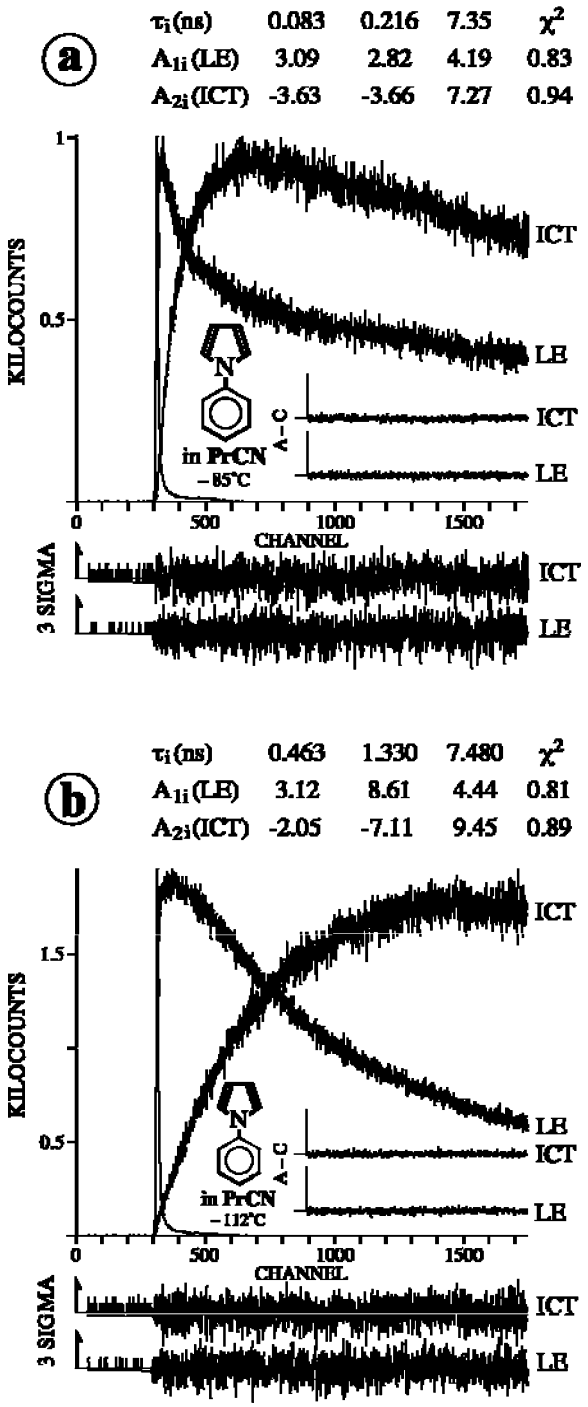

Figure 2. Triple-exponential LE and ICT fluorescence decays of *N*-phenylpyrrole (PP) in *n*-propyl cyanide (PrCN) at (a) −85 °C and (b) −112 °C. The decay times τ_3, τ_2, and τ_1 with the corresponding amplitudes A_{1i}(LE) and A_{2i}(ICT), see eqs 5 and 6, are given in the figure. The shortest decay time is listed first. The weighted deviations sigma, the autocorrelation functions A−C, and the values for χ^2 are also indicated. Emission wavelengths λ_{em}: 303 nm (LE), 400 nm (ICT)). Excitation wavelength λ_{exc}: 276 nm. Time resolution: 1.98 ps/channel with a time window of 1650 effective channels. The corresponding LE/ICT decays (not shown, eq 4) are double exponential, with decay times 149 and 417 ps and relative amplitudes 0.79 and 1.0 at −85 °C (a) and 519 and 3216 ps, with relative amplitudes 0.55 and 1.0 at −112 °C (b), see text.

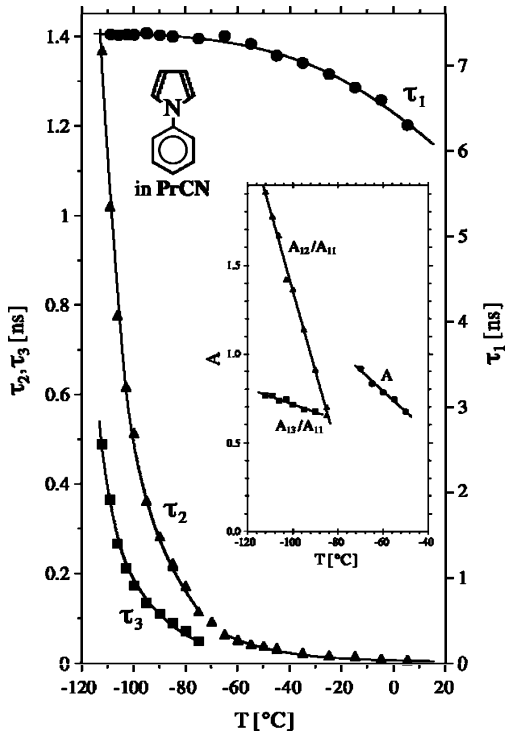

Figure 3. LE and ICT fluorescence decay times of *N*-phenylpyrrole (PP) in *n*-propyl cyanide (PrCN) as a function of temperature (5 to −112 °C). ICT (emission wavelength $\lambda_{em} = 400$ nm) from 5 to −70 °C, LE ($\lambda_{em} = 303$ nm) and ICT (global analysis at $\lambda_{em} = 303$ (LE) and 400 (ICT) nm, as in Figure 2) from −45 to −112 °C. The amplitude ratios A_{13}/A_{11} and A_{12}/A_{11}, see eqs 5 and 6, between −85 and −112 °C are shown in the inset, together with the ratio A of the double-exponential decays between −45 and −70 °C (eqs 1−3). Excitation wavelength λ_{exc}: 276 nm. Time resolution: 1.98 ps/channel with a time window of 1650 effective channels.

Time-Resolved LE and ICT Spectra of PP in PrCN at −100 °C. Contour Plots. By normalizing the 19 fluorescence decays discussed in the previous section with the photostationary dual (LE + ICT) fluorescence spectrum $I_s(\tilde{\nu})$ (eq 7) of PP in PrCN at −100 °C, the time development of the fluorescence spectrum after excitation was reconstructed by making cuts at constant time through the complete data set consisting of the fluorescence intensity as a function of wavelength and time.[21] The fluorescence decays were fitted with 2 or 3 exponentials for each emission wavelength. The total LE + CT fluorescence spectrum at a time delay t after excitation, $0 \le t \le 50$ ns, was calculated by using eq 7 ($n = 2, 3$).

$$I(\tilde{\nu},t) = I_s(\tilde{\nu})\frac{\sum_{i=1}^{n} A_i(\tilde{\nu}) \exp(-t/\tau_i(\tilde{\nu}))}{\sum_{i=1}^{n} A_i(\tilde{\nu})\, \tau_i(\tilde{\nu})} \qquad (7)$$

As examples, the time-resolved fluorescence spectra of PP at three different delay times after excitation (data points) are depicted in Figure 5. In a second step, the LE and ICT contributions to the dual emission spectra in this figure are obtained by spectral subtraction of the time-resolved spectrum with the separated LE fluorescence band of *N*-phenylpyrrole in PrCN at −100 °C (Figure 6a). It is assumed in this procedure that the position of LE band does not depend on time, due to the small dipole moment of PP, in the ground as well in the LE state (1.39 and 1.5 D).[3]

The small difference of 140 cm^{-1} between the ICT emission maximum $\tilde{\nu}^{max}$(ICT) of the photostationary spectrum (27 640 cm^{-1}) and that at infinite time (27 780 cm^{-1}) may be due to the assumption used in the spectral subtraction procedure that the maximum and shape of the LE emission band does not depend on time.

The time development of the LE and ICT emission bands of PP is presented in Figure 6b and Figure 6c, in the form of contour plots of their fluorescence intensity. The contour plots for the LE and ICT bands were constructed from a set of 45 time-resolved LE and ICT fluorescence spectra $I(\tilde{\nu},t)$ (eq 7) by MATLAB (version 7) subroutine CONTOUR. It is seen from these plots that the ICT emission maximum $\tilde{\nu}^{max}$(ICT) (dashed line) undergoes a red-shift of 1450 cm^{-1} (from 29 230 at $t = 0$ (extrapolated) to 27 780 cm^{-1} at infinite time), see Figures 6b and S2 (Supporting Information), whereas the maximum of the LE fluorescence band (Figure 6c) was kept fixed in the spectral analysis, as mentioned above. This spectral shift of $\tilde{\nu}^{max}$(ICT) is a clear indication of the influence of dielectric solvent relaxation, which means that ICT takes place in nonequilibrated solvent surroundings.

Time Development of the ICT Emission Maximum and the ICT and LE Band Integrals. The time dependence of the spectral position of the emission maximum $\tilde{\nu}^{max}$(ICT) of PP in PrCN at −100 °C is presented in Figure 7a. Similarly, the time development of the band integrals BI(LE) and BI(ICT) of the LE and ICT emission bands (see Figure S2 in the Supporting Information) are depicted in Figure 7b and Figure 7c. The decay

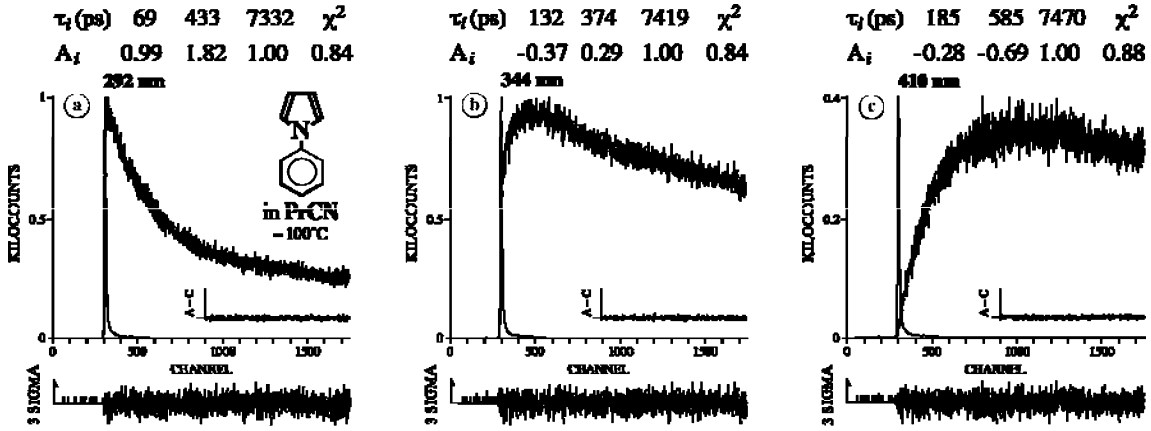

Figure 4. Triple-exponential fluorescence decays of *N*-phenylpyrrole (PP) in *n*-propyl cyanide (PrCN) at −100 °C, with the decay times (τ_3, τ_2, τ_1) and the corresponding amplitudes A_i (eqs 5 and 6) for three different emission wavelengths, 292 (LE), 344 (LE + ICT), and 410 nm (ICT), spanning the fluorescence spectrum (see Figure 1b, at −112 °C). The longest time τ_1, obtained from the analysis of the corresponding decays with 10 ps/channel, is kept fixed in the fitting. The decay times are similar to those determined from a global analysis of the LE and ICT curves at −100 °C (see Figure 3). Excitation wavelength λ_{exc}: 276 nm. Time resolution: 1.98 ps/channel with a time window of 1650 channels. See the caption of Figure 2. A global analysis of the LE and ICT decays is shown in Figure S1 (Supporting Information).

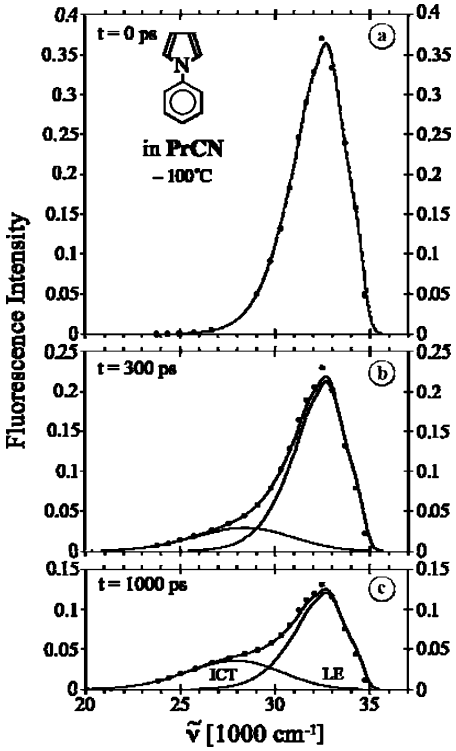

Figure 5. Time-resolved fluorescence spectra (data points) of *N*-phenylpyrrole (PP) in *n*-propyl cyanide (PrCN) at −100 °C for three delay times. The time-resolved spectrum at $t = 0$ (a), without an ICT contribution, is identical to the separated photostationary LE emission (see Figure 1 and text). The line through the data points in (a) and (b) is the sum of the LE and ICT spectra. With increasing delay time, (b) and (c), the LE intensity decreases, with a simultaneous increase of the intensity of the ICT fluorescence band. Note the red-shift of the ICT emission maximum with time: $\tilde{\nu}^{max}$(ICT) = 28 400 cm^{-1} at t = 300 ps and 27 910 cm^{-1} at $t = 1000$ ps, no ICT at $t = 0$. See Figures 6, 7, and S2.

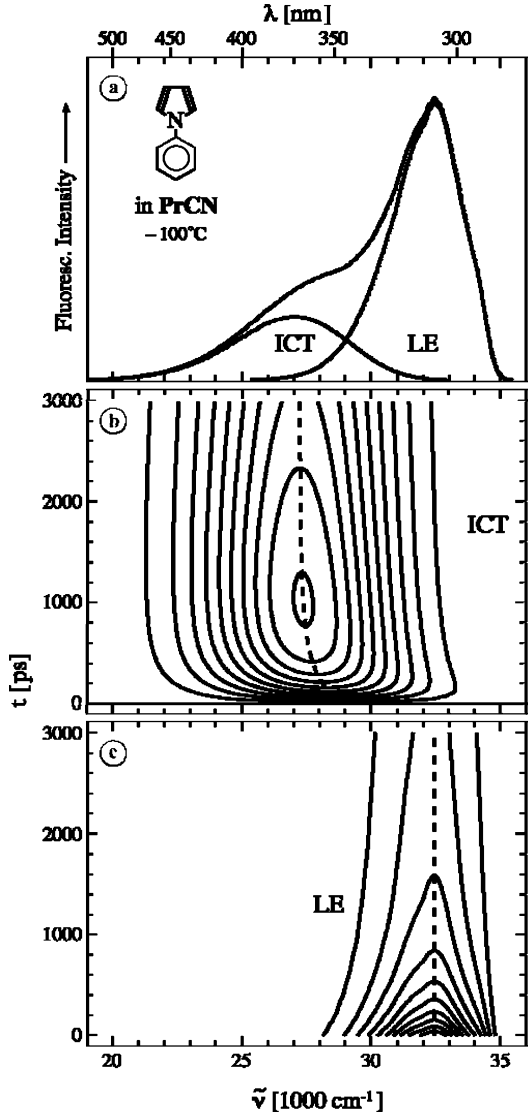

Figure 6. *N*-Phenylpyrrole (PP) in *n*-propyl cyanide (PrCN) at −100 °C. (a) LE and ICT photostationary fluorescence spectra. For the separation of the overall fluorescence spectrum into the LE and ICT components, see Figure 1. (b) Contour plot for the time development of the ICT fluorescence band. The spectral shift of the ICT emission maximum $\tilde{\nu}^{max}$(ICT), from 29 230 to 27 780 cm^{-1}, is indicated by a dashed line. (c) Contour plot for the time development of the LE fluorescence band. The LE emission maximum $\tilde{\nu}^{max}$(LE), dashed line, does not change with time. For the spectral subtraction, the separated LE emission spectrum of PP in PrCN at −100 °C is employed, see Figure 5 and text. The 10 (LE) and 11 (ICT) solid contour lines for the time-resolved ICT and LE emission spectra are the cross sections for the ICT or LE fluorescence hypersurfaces (maximum intensity 0.358 for LE and 0.0355 for ICT) and a horizontal plane at different heights with equal steps (0.0325 for LE and 0.0351 for ICT) starting from 0.0325 for LE and 0 for ICT. Excitation wavelength 276 nm. See also Figure S2 in the Supporting Information.

curves of $\tilde{\nu}^{max}$(ICT), BI(LE), and BI(ICT) are fitted simultaneously with a sum of exponentials $\sum A_i \exp(-t/\tau_i)$, as shown by the lines through the data points in Figure 7. The decay parameters, times τ_i and amplitudes A_i, obtained from this global analysis are listed in Table 2. The time dependence of the spectral position of $\tilde{\nu}^{max}$(ICT) can be fitted as a double exponential with the decay times $\tau_3 = 119$ ps and $\tau_2 = 456$ ps (Table 2). From this global analysis, the same decay times of 119 and 456 ps obviously also result for BI(LE) and BI(ICT), together with the long decay time τ_1 of 7360 ps (Table 2). This last long decay time represents effectively the ICT lifetime and is clearly beyond the time range of the dielectric solvent relaxation (τ_3 and τ_2) that determines the shift of $\tilde{\nu}^{max}$(ICT). The time dependence of the spectral solvation response function $C(t)$,[22] of identical shape as the spectral time shift of $\tilde{\nu}^{max}$(ICT) (see eq 8), is indicated on the right axis of Figure 7a:

$$C(t) = \frac{\tilde{\nu}(t) - \tilde{\nu}(\infty)}{\tilde{\nu}(0) - \tilde{\nu}(\infty)} \tag{8}$$

where $\tilde{\nu}(0)$, $\tilde{\nu}(t)$, and $\tilde{\nu}(\infty)$ are the wavenumbers of the emission maxima at time zero, t, and infinity, respectively.

The deviation from the double-exponential character of the LE and ICT fluorescence decays observed here for PP in PrCN at −100 °C is attributed to the mutual interference of the ICT reaction and the solvent dielectric relaxation. Based on the observation of triple-exponential LE and ICT fluorescence decays, this conclusion is assumed to hold over the entire temperature range from −70 to −112 °C. Our present finding that dielectric solvent relaxation interferes with the ICT reaction of PP in PrCN at temperatures below −70 °C, whereas for PP in EtCN the LE and ICT fluorescence decays are still double exponential at −90 °C,[4] is due to the faster solvent relaxation in the latter solvent. This phenomenon is related to the corresponding decrease in viscosity: 4.86 cP for PrCN as compared with 2.39 cP for EtCN at −90 °C.[25] As data for the temperature dependence of the dielectric relaxation of PrCN were not available at the time,[23] this dependence was studied employing the solvent probe DCS, as reported in the following section.[9−12]

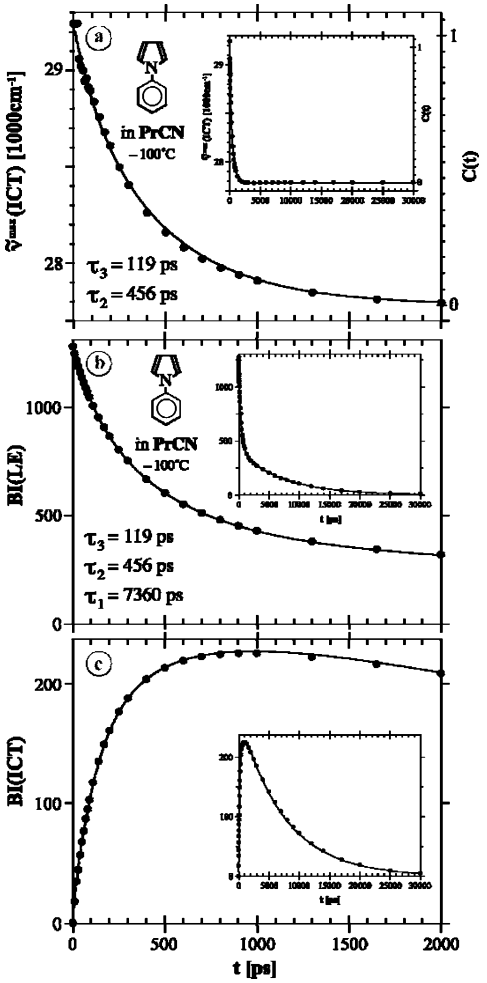

Figure 7. The temporal development of (a) the ICT emission maxima $\tilde{\nu}^{max}$(ICT), see Figures 5, 6b, and S2b (Supporting Information), and the band integrals (BI) over the LE (b) and ICT (c) emission bands of *N*-phenylpyrrole (PP) in *n*-propyl cyanide (PrCN) at −100 °C for a time window of 2000 ps, with a larger time range (0 to 30 ns) as insets. The time-dependent spectral shift of $\tilde{\nu}^{max}$(ICT) is identical in shape to the spectral solvation response function $C(t)$, eq 8. The lines through the data points are calculated from the global analysis of the time dependence of $\tilde{\nu}^{max}$(ICT) together with that of the band integrals BI(LE) and BI(ICT). The decay of $\tilde{\nu}^{max}$(ICT) in (a) can be fitted as a double exponential, with decay times 119 and 456 ps, equal (global analysis) to the times τ_2 and τ_3 for BI(LE) in (b) and BI(ICT) in (c). The decay times (τ_3, τ_2, τ_1) are 119, 456 and 7360 ps, with the corresponding amplitudes 0.50, 1.66 and 1.00 for BI(LE) and −0.51, −0.47 and 1.00 for BI(ICT), see Table 2 and text.

Dielectric Solvent Relaxation of *n*-Propyl Cyanide (PrCN) Measured with DCS. The dielectric solvent relaxation of PrCN at temperatures between −110 and −45 °C was studied employing DCS as the probe molecule.[8−12] DCS is a reliable probe for picosecond solvation processes. After relaxation in the subpicosecond time domain, its photophysics is governed by a single excited state S_1, as already mentioned in the Introduction.[9−12]

The solvent relaxation dynamics of DCS is monitored from the decay of the spectral solvation response function $C(t)$, eq 8, determined from the time-resolved fluorescence spectra. These spectra of DCS are constructed by measuring fluorescence decays $I(t)$ over the fluorescence spectrum (16 decays from 454 to 604 nm, at 10 nm intervals), using the same procedure as described above for the fluorescence decays of PP in PrCN at −100 °C. The time-resolved emission spectra $I(\tilde{\nu},t)$, eq 7, are then calculated over the time interval between 0 and 2 ns. The decay of the solvation response function $C(t)$ of DCS in PrCN at −100 °C, constructed from 26 time-resolved fluorescence spectra of which some are shown in Figure 8, can be fitted as a sum of two exponentials $\sum A_i \exp(-t/\tau_i)$, $i = 1$ and 2. The decay times are 20 (τ_2) and 138 (τ_1) ps, with amplitudes 0.66 and 0.34, see Figure 8 and Tables 2 and 3. These decay times are considered to be the dielectric relaxation times of PrCN at this temperature. The decay of the spectral shift of the fluorescence maximum $\tilde{\nu}^{max}$(flu) of DCS, indicated on the right axis of Figure 8, is in fact (eq 8) identical in shape to that of $C(t)$.

TABLE 2: Decay Times τ_i and Amplitudes A_i of the Multiexponential Decays $\sum A_i \exp(-t/\tau_i)$, $i = 1-n$, for *N*-Phenylpyrrole (PP) in *n*-Propyl Cyanide (PrCN) at −100 °C, Obtained from a Global Analysis of the Decay Functions of the ICT Emission Maximum $\tilde{\nu}^{max}$(ICT) ($n = 2$) and the Band Integrals BI(LE) and BI(ICT) ($n = 3$)[a]

τ_i and A_i	$\tilde{\nu}^{max}$(ICT)[b]	BI(LE)	BI(ICT)	LE + ICT[c]	$C(t)$ (DCS)[d]
τ_1 [ps]	−	7360	7360	7360	−
A_1	−	1.00	1.00	1.00	−
τ_2 [ps]	456	456	456	514	138
A_2	1180[e]	1.66	−0.47	1.364	480[e]
τ_3 [ps]	119	119	119	173	20
A_3	270[e]	0.50	−0.51	0.713	940[e]

[a] See Figure 7. For comparison, the data for the triple-exponential LE + ICT fluorescence decay of PP and the double-exponential spectral solvation response function $C(t)$, eq 8, of 4-dimethylamino-4′-cyanostilbene (DCS) at −100 °C (Figure 8) are also listed. [b] At infinite time, $\tilde{\nu}^{max}$(ICT) of PP equals 27 780 cm^{-1}. [c] Global analysis of the LE and ICT fluorescence decays, see Figure 3. [d] At infinite time, $\tilde{\nu}^{max}$(flu) of DCS equals 18 680 cm^{-1}. [e] In cm^{-1}.

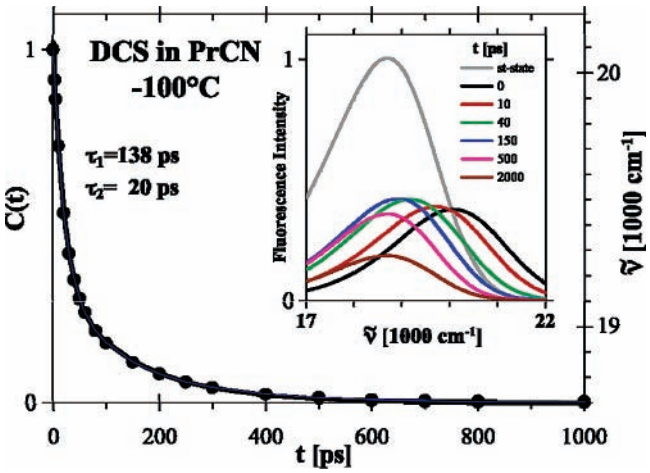

Figure 8. Double-exponential decay $\sum A_i \exp(-t/\tau_i)$ of the spectral solvation response function $C(t)$ (eq 8) of 4-dimethylamino-4′-cyanostilbene (DCS) in *n*-propyl cyanide (PrCN) at −100 °C. The decay times are 20 (τ_2) and 138 ps (τ_1), with amplitudes 0.66 and 0.34 (Table 3). The inset shows the photostationary fluorescence spectrum (maximum at 18 700 cm-1) and the time-resolved emission spectra for delay times t from 0 to 2000 ps after excitation. The maximum $\tilde{\nu}^{max}$(flu) of the fluorescence spectra, with a time dependence identical in shape with that of $C(t)$, is indicated on the right-hand axis: 20 100 cm^{-1} at $t = 0$ and 18 680 cm^{-1} at $t = \infty$: a total spectral shift of 1420 cm^{-1}.

Comparison of Decay Times of PP and DCS in PrCN at −100 °C. A comparison of the two dielectric solvent relaxation times (20 and 138 ps) determined by DCS in PrCN at −100 °C with the two shortest decay times (119 and 456 ps) obtained for the relaxation times of PP in PrCN at this temperature is of interest, see Figures 8 and 9 (Table 2). The similarity of the time of 119 ps (τ_3) of PP and the long solvent relaxation time of 138 ps measured with DCS clearly reveals that the appearance of a third decay time (τ_3) in the fluorescence decays for PP at temperatures below −70 °C in PrCN (Figure 3) is due to solvent relaxation. Also the middle time (τ_2) in these decays is affected

TABLE 3: Decay Times τ_i and Their Amplitudes A_i Obtained from the Double-Exponential Analysis of the Spectral Solvation Response Function $C(t)$ of 4-Dimethylamino-4′-cyanostilbene (DCS) in *n*-Propyl Cyanide (PrCN),[a,b] Eq 8, See Figure 9, in a Comparison with Data Derived from Optical Kerr Effect Measurements (Ref 23)

T (°C)	τ_2 [ps]	τ_1 [ps]	A_2	A_1	τ_2(Kerr) [ps]	τ_1(Kerr) [ps]	A_2(Kerr)	A_1(Kerr)
−110	26	237	0.55	0.45				
−100	20	138	0.66	0.34	21.0	95.0	0.16	0.84
−90	13	80	0.64	0.36	14.0	59.5	0.17	0.83
−80	9	47	0.76	0.24	9.7	38.8	0.18	0.82
−70	9	41	0.88	0.12	7.2	27.1	0.19	0.81
−60	8	34	0.90	0.10	5.8	20.7	0.20	0.80
−45		15[c]		1.00	4.8	15.5	0.21	0.79

[a] Relaxation times (amplitudes) at room temperature: 4.5 (0.71) ps + 1.9 (0.29) ps from optical Kerr effect measurements (ref 23, 296.7 K) and solvent relaxation times τ_S between 1.5 and 2.1 ps from coumarine probes (ref 22). [b] In Table 2, the times τ_2 and τ_1 and their amplitudes A_2 and A_1 are labeled τ_3 and τ_2 (A_3 and A_2), due to the comparison of the DCS data with the triple-exponential decays of BI(LE), BI(ICT), and the LE + ICT fluorescence decays. [c] Single-exponential decay. For the optical Kerr effect data, the mean decay time is 13.3 ps.

by the interference between the ICT reaction of PP and the solvent relaxation of PrCN, see below. The long time τ_1 (around 7 ns) is definitely outside the time range affected by solvent relaxation, as seen from the absence of this time in the temporal shift of $\tilde{\nu}^{max}$(ICT) for PP in PrCN (Figure 7).

Temperature Dependence of the Dielectric Solvent Relaxation Times of PrCN Determined with DCS. The solvation reponse function $C(t)$ was determined with DCS in PrCN at seven temperatures between −110 and −45 °C. The relaxation times with their amplitudes are presented in Figure 9 and Table 3. These times represent the dielectric relaxation times of the solvent PrCN. The results at temperatures above −80 °C are considered to be of limited accuracy, in view of the experimental time resolution, due to the shortening of the solvent relaxation times with increasing temperature. The data, nevertheless, indicate the trend of the temperature dependence of the relaxation times. At −45 °C and higher temperatures, the dielectric relaxation is in fact too fast to be measured with picosecond SPC and will hence not interfere with the ICT reaction of PP in PrCN. This can also be seen from the total spectral shift, which is around 37 nm at −100 °C, but only 6 nm at −45 °C.

Comparison of DCS Relaxation Times with Optical Kerr Effect Results. The recently reported relaxation times of PrCN determined by using ultrafast optical Kerr effect measurements[23] are included in Table 3 for comparison. At −100 °C (extrapolated from −97.5 °C), as an example, the decay times are 21 and 95 ps with amplitudes 0.16 and 0.84. Whereas the first time is the same as that (20 ps) obtained here with DCS, the longer time is clearly shorter than our τ_1 of 138 ps at this temperature. A similar situation is found for the other temperatures for which DCS data are available (Table 3). The reasons for this discrepancy are not clear. A similar difference in relaxation times was noticed previously in a comparison between $C(t)$ and optical Kerr effect data.[24]

Kinetic and Thermodynamic Data from Double-Exponential LE and ICT Fluorescence Decays of PP in PrCN (−45 to −70 °C). Over the temperature range from −70 to 5 °C, the ICT fluorescence decays of PP in PrCN are double exponential (eqs 1−3), see Figure 3. A global analysis of the LE and ICT fluorescence decays between −70 and −45 °C likewise results in two exponentials (Table 4), as already

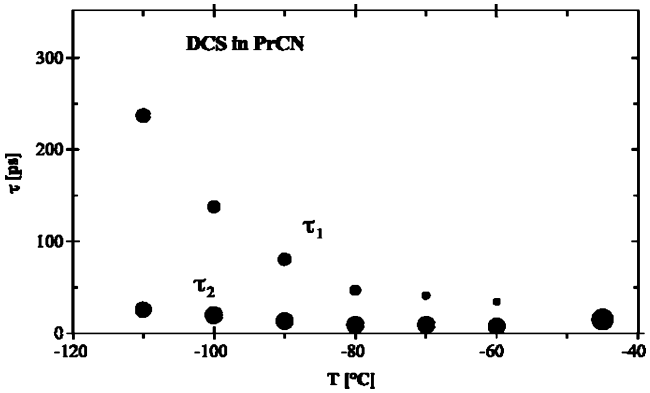

Figure 9. Temperature dependence of the decay times τ_1 (upper dots) and τ_2 (lower dots) for the double-exponential decay $\sum A_i \exp(-t/\tau_i)$ of the spectral solvation response function $C(t)$, eq 8, for 4-dimethylamino-4′-cyanostilbene (DCS) in *n*-propyl cyanide (PrCN). The value of the amplitudes A_i is indicated by the relative size of the data points (Table 3).

reported for −45 °C.[4] In accordance with this observation of two decay times, the LE/ICT decays (eq 4) are single exponential over this temperature range (Table 4).

From an analysis of the decay times τ_1 and τ_2, the amplitude ratio A (eqs 1−3) and the lifetime τ_0(LE) of the model compound PP4M (no ICT),[3] the ICT rate constants k_a and k_d, as well as the lifetime τ'_0(ICT) of the ICT state, are determined (Scheme 1, eqs 9−11), see Table 4.[4] The results are depicted as an Arrhenius plot in Figure 10.

$$k_a = (1/\tau_1 + A/\tau_2)/(1 + A) - 1/\tau_0(\mathrm{LE}) \quad (9)$$

$$k_d = \{(1/\tau_2 - 1/\tau_1)^2 - (2k_a + 2/\tau_0(\mathrm{LE}) - 1/\tau_1 - 1/\tau_2)^2\}/4k_a \quad (10)$$

$$1/\tau'_0(\mathrm{ICT}) = 1/\tau_1 + 1/\tau_2 - k_a - k_d - 1/\tau_0(\mathrm{LE}) \quad (11)$$

From the slope of the lines through the data points of k_a and k_d in Figure 10, the forward and backward ICT activation energies $E_a = 12.4$ kJ/mol and $E_d = 17.0$ kJ/mol are determined, leading to an ICT stabilization enthalpy ΔH (= $E_a - E_d$) of −4.6 kJ/mol for PP in PrCN (Table 5). From the preexponential factors k_a^0 and k_d^0, $\Delta S = R \ln(k_a^0/k_d^0)$, an entropy difference $\Delta S = -23$ J mol^{-1} K^{-1} between the LE and ICT states is calculated (Table 5). In Table 5, the corresponding data for PP in the more polar alkyl cyanides EtCN and MeCN (taken from ref 4) are also listed, for comparison.

Extrapolation based on the data in Tables 4 and 5 results in decay times τ_2 of 347 ps with $A = 1.36$ for −100 °C and 695 ps with $A = 1.60$ for −112 °C. Inspection of Figure 3 shows that these calculated ICT decay times are in between the two lowest experimental decay times of PP in PrCN, indicating that both times are indeed affected by solvent relaxation.

Thermodynamic Data for PP in Three Alkyl Cyanides. Influence of Solvent Polarity. From the data in Table 5 it is seen that, for the ICT reaction of PP in the three alkyl cyanides PrCN, EtCN, and MeCN, the activation energy E_a of the LE → ICT reaction becomes smaller with increasing solvent polarity, from 12 kJ/mol in PrCN to 6 kJ/mol in MeCN. Such a polarity dependent decrease is not observed for the barrier E_d of the ICT back reaction (Scheme 1), with a mean value of 16 kJ/mol in the three solvents, as the decrease in the energy of the transition state goes parallel with that of the ICT state (Figure 11).

The ICT stabilization energy $-\Delta H$ clearly increases with increasing solvent polarity, 4.6 kJ/mol (PrCN), 6.7 kJ/mol (EtCN), and 10.0 kJ/mol (MeCN), as should be expected for

TABLE 4: Decay Parameters and Rate Constants for the ICT Reaction of *N*-Phenylpyrrole (PP) as a Function of Temperature (−70 to −45 °C) in *n*-Propyl Cyanide (PrCN) Taken from the Global Analysis of the LE and ICT Fluorescence Decays

T (°C)	τ_2 [ps]	τ_1 [ns]	A^a	τ_0(LE) [ns][b]	k_a [10^{10} s^{-1}]	k_d [10^{10} s^{-1}]	k_a/k_d[c]	τ'_0(ICT) [ns]	τ(LC)[d] [ps]	ΔG[e] [kJ/mol]
−70	80.5	7.12	0.917	12.23	0.59	0.63	0.935	4.90	153 (153)[f]	0.11
−65	65.3	7.11	0.832	12.14	0.69	0.82	0.846	4.76	112 (112)	0.29
−60	53.5	7.03	0.783	12.05	0.82	1.03	0.795	4.60	92 (95)	0.41
−55	42.7	6.96	0.744	11.96	1.00	1.33	0.753	4.47	74 (74)	0.51
−50	36.4	6.89	0.674	11.87	1.11	1.62	0.682	4.25	56 (60)	0.72
−45[g]	31.3	7.38	0.71	11.77	1.33	1.85	0.719	4.86	56 (53)	0.63

[a] Equation 3. [b] Fluorescence lifetime of PP4M in PrCN, see text. [c] $k_a/k_d \sim A$ when $\tau_2 \ll \tau_1$ (refs 4, 26) as derived from eq 3. [d] The LE/ICT decay time (eq 4). [e] $\Delta G = -RT \ln(k_a/k_d)$. [f] Value in parentheses calculated with the expression $\tau(\mathrm{LC}) = 1/(k_d + 1/\tau'_0(\mathrm{ICT}))$ (ref 4). [g] Data from ref 4.

TABLE 5: Thermodynamic Data for the ICT Reaction of *N*-Phenylpyrrole (PP) in Propyl Cyanide (PrCN) Taken from the Arrhenius Plots in Figure 10[a]

solvent	ϵ[b]	E_a [kJ/mol]	E_d [kJ/mol]	$-\Delta H$ [kJ/mol][c]	$k_a°$ [10^{12} s^{-1}]	$k_d°$ [10^{12} s^{-1}]	$-\Delta S$[d] [J K^{-1} M^{-1}][e]
PrCN	24.1 (35.1)	12.4 ± 0.6	17.0 ± 1.2	4.6 ± 1.7	9.2 ± 2	150 ± 47	23 ± 12
EtCN[e]	29.2 (39.0)	9.0 ± 0.2	15.7 ± 0.3	6.7 ± 0.2	4.2 ± 0.4	109 ± 17	27 ± 7
MeCN[e]	36.7 (50.2)	5.7 ± 0.3	15.7 ± 0.9	10.0 ± 1.1	2.1 ± 0.3	65 ± 31	28 ± 17

[a] Corresponding data for ethyl cyanide (EtCN) and acetonitrile (MeCN) are listed for comparison. [b] Dielectric constant at 25 °C (at −45 °C in parentheses), as an indication of the relative solvent polarities. [c] $-\Delta H = E_d - E_a$. [d] $\Delta S = R \ln(k_a°/k_d°)$. [e] Data from ref 4.

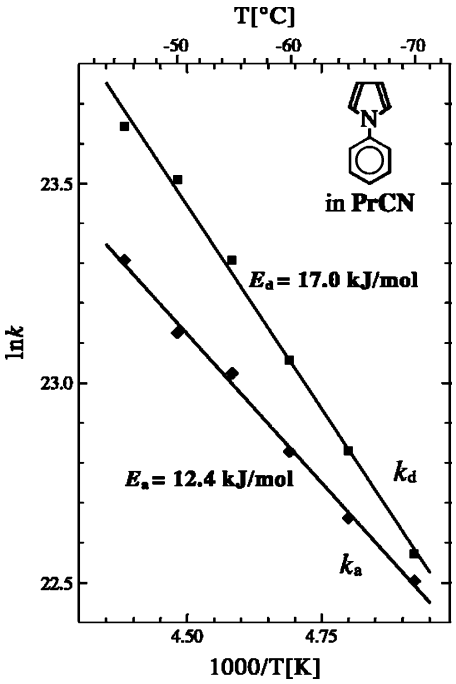

Figure 10. Arrhenius plot of the forward and backward ICT rate constants k_a and k_d (in s^{-1}, Scheme 1), with activation energies E_a and E_d (Table 5), of *N*-phenylpyrrole (PP) in *n*-propyl cyanide (PrCN), calculated from the global analysis of the LE and ICT fluorescence decays between −45 and −70 °C (Table 4).

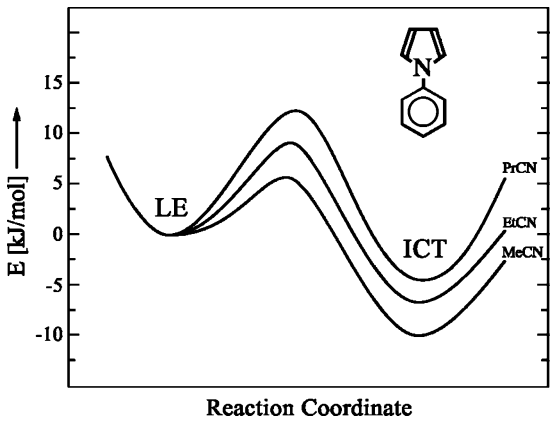

Figure 11. Potential energy surfaces for the reaction between the LE and ICT states of *N*-phenylpyrrole (PP) in *n*-propyl cyanide (PrCN), ethyl cyanide (EtCN), and methyl cyanide (MeCN), showing the decrease of the reaction barrier and the ICT state energy with increasing solvent polarity (Table 5).

an ICT reaction such as with PP, involving a change in the excited-state dipole of 16 D (ICT) during the ICT reaction.[3] The ICT entropy change ΔS of PP in PrCN is strongly negative (−23 J mol^{-1} K^{-1}), similar to what has been observed[4] with PP in the solvent series PrCN to MeCN (Table 5).

ICT Potential Energy Surface. Late Transition State for ICT with PP in Alkyl Cyanides. The observation that for PP in the alkyl cyanides listed in Table 5 the forward ICT barrier E_a clearly decreases with increasing solvent polarity, whereas the barrier E_d for the back reaction remains practically unaffected, indicates that the charge distribution (dipole moment) at the top of the reaction barrier, the transition state, is similar to that of the reaction product: the ICT state. In other words, the ICT reaction of PP in the three alkyl cyanides investigated here has a *late transition state*, as was already concluded for PP in EtCN and MeCN.[4] When the reaction would have an early transition state with a charge distribution similar to that of the LE state, the forward ICT barrier E_a would be expected to be largely independent of solvent polarity. This conclusion is opposite to that reached for the ICT reaction of DMABN in MeCN.[27] Such an early transition state cannot easily be reconciled with the observation that the barrier E_a of DMABN strongly decreases with increasing solvent polarity,[14,16,28] similar to what is found here for PP.

The occurrence of a late transition state means that this state has a relatively large dipole moment, similar to the 13 D of the ICT state.[3] As the magnitude of μ_e(ICT) is directly controlled by the change in the molecular configuration of PP, the molecular structure of the transition state will be similar to that of the ICT, although the transition state is closer in energy to the LE than to the ICT state (Figure 11).

Leffler−Hammond Postulate and the ICT Reaction of PP. According to a strict interpretation of the Leffler−Hammond postulate,[29−32] the difference in energy between the reactant or product and the transition state determines whether an early (similar structure as the reactant) or late (similar to product) transition state is involved in a reaction. Under the thermodynamic circumstances encountered here for the ICT reaction with PP in the alkyl cyanides ($E_a < E_d$, i.e., $\Delta H < 0$: see Table 5

and Figure 11), this postulate would lead to the conclusion that an early (LE-like) transition state must be present, with a charge distribution or dipole moment similar to that of LE. This expectation is in line with the general assumption, that exothermic reactions have late transition states, irrespective of the precise molecular nature of the reaction.[33] For an early transition state, E_a would be more or less independent of solvent polarity, whereas E_d should become larger when going from PrCN to MeCN because of increasing solvent polarity, clearly contrary to observations presented here. Several exceptions to the Leffler−Hammond postulate have been reported and discussed in the literature.[34−37] Sometimes the terminology "anti-Hammond behavior" is used in this connection.[35,37] The characterization as "late" of the transition state for the ICT reaction with PP in the alkyl cyanides is governed primarily by its charge distribution (dipole moment) rather than by its energy relative to that of the reactant (LE) or the product (ICT).

Conclusions

The LE and ICT fluorescence decays of PP in PrCN are double exponential from 5 to −70 °C, whereas below this temperature three exponentials are required, down to the melting point of the solvent (−112 °C). This means that over this lower temperature range the ICT kinetics is more complex than that based on the two excited states LE and ICT (Scheme 1). The appearance of triple-exponential decays is caused by dielectric solvent relaxation of PrCN, which slows down upon cooling and then starts to interfere with the ICT of PP. The reason that this complication appears in PrCN and not in the alkyl cyanides EtCN and MeCN is due to the higher viscosity[25] and hence slower dielectric response of the former solvent. The solvent relaxation for PP in PrCN at −100 °C is determined from time-resolved LE and ICT emission spectra. The decay of the solvent response function $C(t)$, in fact the spectral shift of the maximum of the ICT fluorescence band, results in the two exponentials 119 and 456 ps and covers a spectral shift of 1450 cm^{-1}, reflecting the time needed for the equilibration of the ICT state and the total spectral red-shift involved. With the solvent polarity probe DCS, the dielectric relaxation times 20 and 138 ps are obtained for PrCN at −100 °C, of which the latter is similar to the shortest solvent response time (119 ps) measured with PP. This similarity supports the interpretation that dielectric solvent relaxation is responsible for the complex fluorescence decay of PP in PrCN below −70 °C.

The ICT kinetics of PP in PrCN is analyzed from the double-exponential LE and ICT decays measured between −45 and −70 °C. The forward ICT barrier E_a (12.4 kJ/mol) is clearly larger than those previously reported for the more polar alkyl cyanides EtCN (9.0 kJ/mol) and MeCN (5.7 kJ/mol), whereas the barrier E_d (17.0 kJ/mol) for the ICT → LE reaction is largely polarity independent, similar to that in EtCN and MeCN (16 kJ/mol). These results show that the ICT reaction of PP in the investigated alkyl cyanides has a late transition state with a charge distribution similar to that of the ICT state.

Acknowledgment. Mr. J. Bienert, Mr. W. Bosch, and Mr. H. Lesche are thanked for expert technical assistance. We are grateful to Prof. J. Fourkas for measuring the dielectric behavior of PrCN and other alkyl cyanides as a function of temperature (ref 23).

Supporting Information Available: Double and triple exponential fluorescence decays (LE and ICT) of PP in PrCN at −100 °C (Figure S1). Temporal development of the LE and ICT fluorescence bands of PP in PrCN at −100 °C, showing the influence of dielectric solvent relaxation (Figure S2). This material is available free of charge via the Internet at http://pubs.acs.org.

References and Notes

(1) Rettig, W.; Marschner, F. *Nouv. J. Chim.* **1983**, *7*, 425.

(2) Rettig, W.; Marschner, F. *New J. Chem.* **1990**, *14*, 819.

(3) Yoshihara, T.; Galievsky, V. A.; Druzhinin, S. I.; Saha, S.; Zachariasse, K. A. *Photochem. Photobiol. Sci.* **2003**, *2*, 342.

(4) Yoshihara, T.; Druzhinin, S. I.; Demeter, A.; Kocher, N.; Stalke, D.; Zachariasse, K. A. *J. Phys. Chem. A* **2005**, *109*, 1497.

(5) Cogan, S.; Zilberg, S.; Haas, Y. *J. Am. Chem. Soc.* **2006**, *128*, 3335.

(6) Zilberg, S.; Haas, Y. *J. Phys. Chem. A* **2002**, *106*, 1.

(7) Xu, X.; Cao, Z.; Zhang, Q. *J. Phys. Chem. A* **2006**, *110*, 1740.

(8) Gruen, H.; Görner, H. *Z. Naturforsch.* **1983**, *38A*, 928.

(9) Il'ichev, Yu. V.; Kühnle, W.; Zachariasse, K. A. *Chem. Phys.* **1996**, *211*, 441.

(10) Il'ichev, Yu. V.; Zachariasse, K. A. *Ber. Bunsen-Ges. Phys. Chem.* **1997**, *101*, 625.

(11) Kovalenko, S. A.; Schanz, R.; Senyushkina, T. A.; Ernsting, N. P. *Phys. Chem. Chem. Phys.* **2002**, *4*, 703.

(12) Arzhantsev, S.; Zachariasse, K. A.; Maroncelli, M. *J. Phys. Chem. A* **2006**, *110*, 3454.

(13) Amatatsu, Y. *J. Phys. Chem. A* **2006**, *110*, 8736.

(14) Druzhinin, S. I.; Ernsting, N. P.; Kovalenko, S. A.; Pérez Lustres, L.; Senyushkina, T.; Zachariasse, K. A. *J. Phys. Chem. A* **2006**, *110*, 2955.

(15) Striker, G. In *Deconvolution and Reconvolution of Analytical Signals*; Bouchy, M., Ed.; University Press: Nancy, France, 1982; p 329.

(16) Zachariasse, K. A.; Kühnle, W.; Leinhos, U.; Reynders, P.; Striker, G. *J. Phys. Chem.* **1991**, *95*, 5476.

(17) Druzhinin, S. I.; Galievsky, V. A.; Zachariasse, K. A. *J. Phys. Chem. A* **2005**, *109*, 11213.

(18) In the case of relatively small Φ′(ICT)/Φ(LE) ratios, such as with PP in PrCN at 25 °C (Figure 1a), separation of the LE and ICT contributions to the overall fluorescence spectrum will not necessarily result in accurate values for Φ′(ICT)/Φ(LE), as the outcome of the subtraction will depend on the procedure followed. For the spectral separation in the present paper, the ICT emission band of 4-cyano-*N*-phenylpyrrole in PrCN has been used, whereas the subtraction employed in ref 4 was based on the LE fluorescence spectrum of 4-methyl-*N*-phenylpyrrole. Even when the resulting values for Φ′(ICT)/Φ(LE) are not exactly the same (see Table 1 and ref 4), the differences in the slope of the plots of ln(Φ′(ICT)/Φ(LE)) vs the reciprocal temperature are small.

(19) Landolt-Börnstein. In *Numerical Data and Functional Relationships in Science and Technology, New Series*; Madelung, O., Ed.; Springer: Berlin, 1991; Vol. 6, Group IV.

(20) Landolt-Börnstein; In *Numerical Data and Functional Relationships in Science and Technology, New Series*; Lechner, M. D., Ed.; Springer: Berlin, 1996; Vol. 38B, Group III.

(21) Dahl, K.; Biswas, R.; Ito, N.; Maroncelli, M. *J. Phys. Chem. B* **2005**, *109*, 1563.

(22) Kahlow, M. A.; Kang, T. J.; Barbara, P. F. *J. Chem. Phys.* **1988**, *88*, 2372.

(23) Zhu, X.; Farrer, R. A.; Zhong, Q.; Fourkas, J. T. *J. Phys.: Condens. Matter* **2005**, *17*, S4105.

(24) Castner, E. W.; Maroncelli, M. *J. Mol. Liq.* **1998**, *77*, 1.

(25) Landolt-Börnstein. In *Numerical Data and Functional Relationships in Science and Technology, New Series*; Lechner, M. D., Ed.; Springer: Berlin, 1996; Vol. 18B, Group IV.

(26) Il'ichev, Yu. V.; Kühnle, W.; Zachariasse, K. A. *J. Phys. Chem. A* **1998**, *102*, 5670.

(27) Fonseca, T.; Kim, H. J.; Hynes, J. T. *J. Photochem. Photobiol. A: Chem.* **1994**, *82*, 67.

(28) Hicks, J.; Vandersall, M.; Sitzmann, E. V.; Eisenthal, K. B. *Chem. Phys. Lett.* **1987**, *135*, 413.

(29) Leffler, J. E. *Science* **1953**, *117*, 340.

(30) Hammond, G. S. *J. Am. Chem. Soc.* **1955**, *77*, 334.

(31) An Interview with G. S. Hammond. *Spectrum* **2004**, *17* (3), 4.

(32) Isaacs, N. *Physical Organic Chemistry*, 2nd ed.; Longman: Harlow, U.K., 1995; Chapter 2.10, p119.

(33) Agmon, N. *J. Chem. Soc., Faraday Trans. 2* **1978**, *74*, 388.

(34) Arnett, E. M.; Reich, R. *J. Am. Chem. Soc.* **1980**, *102*, 5892.

(35) Johnson, C. D. *Tetrahedron* **1980**, *36*, 3461.

(36) Shaik, S. S. *Prog. Phys. Org. Chem.* **1985**, *15*, 197.

(37) Kurz, J. L. *J. Org. Chem.* **1983**, *48*, 5117.